International Journal of General Medicine

Dovepress

open access to scientific and medical research

Open Access Full Text Article

ORIGINAL RESEARCH

Circular RNA circEZH2 Promotes Lung Adenocarcinoma Progression by Regulating microRNA-495-3p/Tumor Protein D52 Axis and Activating Nuclear Factor-Kappa B Pathway

Liping Chen[1], Tongwei Xiang[2], Jing Xing[2], Xinan Lu[2], Shan Wei[2], Huaying Wang[2], Jipeng Li[1], Wanjun Yu[2]

[1]Department of Central Laboratory, The Affiliated People's Hospital of Ningbo University, Ningbo, People's Republic of China; [2]Department of Respiratory and Critical Care Medicine, The Affiliated People's Hospital of Ningbo University, Ningbo, People's Republic of China

Correspondence: Liping Chen; Wanjun Yu, Email Chenliliy@outlook.com; nbyuwanjun@163.com

Background: It has been increasingly recognized that circular RNAs (circRNAs) act as a pivotal factor in the onset and progression of human malignancies. Yet, the specific activities and mechanistic roles of these RNAs in the context of lung adenocarcinoma (LUAD) are not fully understood.

Methods: Microarray analysis identified a novel LUAD-associated circular RNA, termed hsa_circ_0006357 (also referred to as circEZH2). Reverse transcription–quantitative polymerase chain reaction (RT-qPCR) was utilized for the analysis of circEZH2 expression in tissues and cell lines. The characteristics of circEZH2 were verified by RNase R treatment and fluorescence in situ hybridization (FISH) assays. The functions of circEZH2 were detected by Cell Counting Kit-8 (CCK-8), colony formation, wound healing, and Transwell assays. The molecular mechanism of circEZH2 was clarified through bioinformatics analysis as well as RNA pulldown, dual-luciferase reporter, RT-qPCR, and immunoblotting assays. The role of circEZH2 in vivo was investigated using a xenograft model.

Results: This investigation revealed that circEZH2 expression was elevated in LUAD cell lines and tumor samples. This elevation was associated with enhanced cell proliferation, migratory capacity, epithelial–mesenchymal transition (EMT), and invasion in vitro. Conversely, silencing of circEZH2 in vivo resulted in a notable decrease in LUAD tumorigenesis, whereas its overexpression led to the opposite effects. Mechanistically, circEZH2 appeared to act as a sponge for miR-495-3p, facilitating the upregulation of tumor protein D52 (TPD52) and triggering the nuclear factor kappa B (NF-κB) signaling pathway, thus contributing to the progression of LUAD.

Conclusion: These findings indicate that circEZH2 may function as a competitive endogenous RNA (ceRNA), driving the progression of LUAD by manipulating the miR-495-3p/TPD52 axis and activating the NF-κB pathway.

Keywords: lung adenocarcinoma, circular RNA, nuclear factor kappa B, tumor protein D52, miR-495-3p

Introduction

Lung cancer remains one of the deadliest malignancies worldwide. Among the various types, lung adenocarcinoma (LUAD) is the most prevalent form of lung cancer.[1] Although the long-term survival of certain subgroups of LUAD patients has improved due to the advancement of therapeutic tools, the five-year survival rate of patients remains relatively low. Therefore, deeper insights into the molecular mechanisms driving LUAD progression are urgently needed to identify novel intervention points.

Circular RNAs (circRNAs) are novel endogenous RNAs that are characterized by covalently closed loop structures without a 5′-cap and a 3′-poly (A) tail,[2] and they are implicated in crucial roles in the oncogenesis and progression of various cancer types,[3] including LUAD.[4] For instance, research indicates that circ_0004140 acts as a pivotal factor to promote LUAD development and enhance immune system evasion via the circ_0004140/miR-1184/CCL22 signaling pathway.[5] Circ_0088036 promotes LUAD cell growth, invasion, and epithelial–mesenchymal transition (EMT) via

Received: 10 April 2024
Accepted: 13 September 2024
Published: 28 September 2024

modulating the miR-203/SP1 axis in LUAD.[6] These circRNAs possess microRNA (miRNA) response elements that are capable of functioning as miRNA decoys, thereby mitigating miRNA-mediated gene silencing.[7,8] Furthermore, miRNAs have the capacity to associate with the 3′-untranslated region of mRNAs to either inhibit translation or promote mRNA degradation,[9] thus contributing to the complex post-transcriptional landscape of post-transcriptional regulation. Therefore, circRNAs have been recognized as key modulators in miRNA/mRNA axis regulation.[10,11] Nonetheless, the regulatory details of hsa_circ_0006357 (circEZH2) in the context of LUAD remain to be comprehensively uncovered.

Our latest findings highlight a novel circRNA associated with LUAD, circEZH2, which exhibits significant upregulation within LUAD tissues and cell lines. It is crucial for the progression of LUAD that circEZH2 orchestrates the regulation of the miR-495-3p/tumor protein D52 (TPD52) axis and is involved in the activation of the signaling pathway of nuclear factor kappa B (NF-κB) signaling pathway. These insights will pave the way for circEZH2 to be potentially recognized as a novel molecular target for innovative therapeutic strategies against LUAD.

Materials and Methods

Cell Culture

The human bronchial epithelial cell line (BEAS-2B) and three LUAD cell lines (NCI-H1299, A549, and SPC-A1) were purchased from Biobw (Beijing, China). The cells were cultivated in Dulbecco's modified Eagle medium (DMEM, VivaCell, China) containing 1% penicillin-streptomycin (Gibco, USA) and 10% fetal bovine serum (FBS, VivaCell, China) and maintained at 37°C in an incubator supplied with 5% CO_2.

Tissue Acquisition

A total of thirty LUAD samples and the corresponding noncancerous tissues, located 2 cm from the tumor margin, were obtained from individuals undergoing treatment at the Affiliated People's Hospital of Ningbo University.[12] These subjects all had confirmed cases of primary LUAD, with no prior exposure to therapies such as immunotherapy, targeted therapy, or chemotherapy. The LUAD samples were cryopreserved at −80°C until analysis. Informed consents were secured from all participants. This study received approval from the Ethics Committee of the Affiliated People's Hospital of Ningbo University (approval number: 2022012).

Reverse Transcription–Quantitative Polymerase Chain Reaction (RT-qPCR)

Total RNA was isolated from both the tissue samples and BEAS-2B, NCI-H1299, A549, and SPC-A1 cell lines utilizing TRIzol (Invitrogen, USA). Reverse transcription of circRNAs and mRNAs was conducted using Prime Script™ RT Master Mix (Takara, Japan). The qPCR was executed with SYBR Green (TransGen Biotech, China). The miRNA levels were assessed by a miRNA 1st Strand cDNA Synthesis Kit (by Stem-loop) and a microRNA q-PCR kit (Sangon Biotech, China). The primers used for qPCR, developed and manufactured by Sangon Biotech (Shanghai, China), are detailed in Supplementary Table S1. The relative gene expression was evaluated by employing the $2^{-\Delta\Delta Ct}$ method, using glyceraldehyde 3-phosphate dehydrogenase or U6 as the internal standard.[13]

RNase R Treatment

Total RNA isolated from SPC-A1 and A549 cells was treated with 3 U/μg RNase R (Beyotime, China), followed by a 30-min incubation at 37°C. Next, RT-qPCR was carried out to assess the expression levels of circEZH2 and EZH2. This procedure was replicated three times for accuracy.

Fluorescence in situ Hybridization (FISH)

The FISH detection was processed with a kit (GenePharma, China), according to the manufacturer's protocol. For the hybridization, a Cy3-labeled circEZH2 probe (sequence: 5′-CATGATTATTCTCCCTAGTCCCG-3′; GenePharma, China) was used. The cells were reacted with the probe overnight at 37°C. After hybridization, nuclear staining was performed by 4′,6-diamidino-2-phenylindole (DAPI), and fluorescence images were taken on a Leica DM4B microscope (Leica DM4B, Germany).

Transfection

Small interfering RNAs (siRNAs) targeting circEZH2 (si-circEZH2-1 through si-circEZH2-5), a negative control siRNA (si-NC), an overexpression plasmid for circEZH2 (pEX-3-circEZH2), its corresponding control plasmid (pEX-3), miR-495-3p mimics, and the miRNA mimic negative contrast (miR-NC) were produced by GenePharma (Shanghai, China). TPD52 siRNAs and the negative control siRNA were prepared by keyGEN BioTECH (Jiangsu, China). These RNAs and plasmid molecules were transfected into SPC-A1 and A549 cells using Lipofectamine 2000 (Invitrogen, USA) and harvested 48 h later. The targeted oligonucleotide sequences are listed in Supplementary Table S2.

Cell Counting Kit (CCK)-8 Assay

For the CCK-8 examination, 3000 cells were seeded in each well of 96-well plates and cultivated under standard conditions. A 10-μL sample of CCK-8 solution (Transgen, China) was dropped into each well after 0, 24, 48, and 72 h. Subsequently, the absorbance at 450 nm was read by a microplate reader to assess cell viability.

Colony Formation Assay

A total of 500 transfected cells were seeded into each well of 6-well plate with DMEM supplemented with 10% FBS. Following a 14-day incubation, the colonies were fixed using methanol and then stained with 1% crystal violet (Sangon Biotech, China). The colony numbers were then counted manually.

Wound Healing Assay

To determine cellular migration, 300,000 LUAD cells subjected to specific treatments were seeded in a well of a six-well plate. After 24 h, a linear wound was created using a 200-μL pipette tip. Cellular migration was calculated from the images captured at 0 h and 24 h using an inverted microscope (Nikon Corporation). This assay was repeated independently three times.

Transwell Assay

A total of 50,000 transfected cells were seeded into chambers coated with Matrigel (BD Bioscience, USA) and serum-free medium. These chambers were placed into a 24-well plate containing DMEM with 20% serum. After 24 h, 4% paraformaldehyde (Solarbio, China) and 0.1% crystal violet were applied for the fixing and staining of the invading cells on the lower surface membrane. The number of cells was then counted under an optical microscope (Nikon Corporation).

RNA Pull-Down Assay

The interactions between circEZH2 and various miRNAs, including miR-1265, miR-495-3p, miR-554, and miR-556-5p, were explored using an RNA precipitation assay. The biotin-associated circEZH2 (GenePharma, China) probes were mixed with streptavidin magnetic beads and incubated at room temperature for 2 h. Lysates of A549 and SPC-A1 were prepared using radioimmunoprecipitation assay (RIPA) buffer and incubated overnight with the bead-bound probes at 4°C. This was followed by washing and RT-qPCR to detect the bound miRNAs.

Dual-Luciferase Assay

We cloned both the mutant miR-495-3p binding sites and wild-type circEZH2 into the *Renilla pGL3 vector* (Promega, USA) and transfected them into A549 and SPC-A1 cells along with the miR-495-3p mimics or control mimics. The luciferase activity was assessed with a Dual-Luciferase Reporter Assay System (Promega, Madison, USA) after 48 h.

In-Vivo Xenograft Experiments

Adhering to the guidelines of Ningbo University's Animal Experimental Research Ethics Committee (approval no. 11332), animal studies were conducted. The circEZH2-knockdown virus and circEZH2-overexpression vectors were generated and introduced into LUAD cells. Stable cell lines were selected using puromycin or G418. These engineered cells were then injected into male BALB/c nude mice (six per group). The tumor volume was calculated every three days. After four weeks, the mice were euthanized, and the tumors were excised and weighed.

Immunohistochemical Analysis

Following fixation in 4% paraformaldehyde, xenograft tissues were paraffin-embedded and sectioned. The sections were then reacted with a ki-67 antibody (Abcam, USA) and a secondary biotinylated anti-rabbit antibody, followed by incubation with 3,3′-diaminobenzidine detection (Vectorlab, USA), as per the manufacturers' protocols.

Immunoblotting Analysis

Protein from cells and tissues was extracted using RIPA buffer (Beyotime, Shanghai, China), separated by sodium dodecyl sulfate–polyacrylamide gel electrophoresis, and transferred to a polyvinylidene difluoride membrane. The membranes were reacted overnight with primary antibodies targeting specific proteins, including β-actin, E-cadherin, vimentin, TPD52, NF-κB p65, and Phospho-NF-κB p65 (Ser536), and incubated with secondary antibodies. The probed proteins were visualized by staining with an enhanced chemiluminescence substrate (Bio-Rad, USA) and quantified using ImageJ software. The antibodies used in this study are listed in Supplementary Table S3.

Statistical Analysis

All collected experimental data were expressed as the mean±standard deviation (SD) calculated by GraphPad Prism 7.0 (GraphPad Software, Boston, MA, USA). These results represent the findings calculated by a minimum of three independent assays. The Student's *t*-test was employed to analyze the differences between two distinct groups. For analyzing differences among multiple groups, analysis of variance with Bonferroni's post-hoc analysis was utilized. The association between the levels of circEZH2 and clinical features was assessed using Fisher's exact test. Pearson's correlation coefficient was also employed to evaluate the correlation in expression between miR-495-3p, circEZH2, and TPD52 mRNAs in LUAD tissue samples. A *p*-value of less than 0.05 was considered as statistically significant.

Results

CircEZH2 is Upregulated in LUAD

A comprehensive circRNA microarray study using three matched pairs of LUAD and adjacent nontumor tissue was conducted to identify circRNAs with differential expression. This study revealed a significant upregulation of hsa_circ_0006357 (circEZH2) in LUAD tissue compared to normal tissue (Figure 1A), suggesting its potential role in the progression of LUAD. Subsequent verification via RT-qPCR on 30 paired LUAD and nontumorous tissues confirmed the higher expression of circEZH2 in cancerous tissues (Figure 1B). Additionally, an examination of the association between circEZH2 expression and clinical parameters in these 30 LUAD patients showed a significant association with the TNM stage (p=0.0110) (Table 1). Comparison of LUAD cell lines (NCI-H1299, A549, and SPC-A1) with normal BEAS-2B cells also showed an elevated level of circEZH2 in cancer cells (Figure 1C). Moreover, resistance of circEZH2 to RNase R digestion was observed, in contrast to the degradation of linear EZH2 (Figure 1D). Furthermore, the cellular localization of circRNA, predominantly in the cytoplasm, was identified via FISH (Figure 1E). Collectively, these findings indicate the stable nature and potential involvement of circEZH2 in LUAD development.

CircEZH2 Promotes LUAD Cellular Proliferation in vivo and in vitro

The biological impact of circEZH2 in LUAD cells was explored using specific siRNAs for gene knockdown and a full-length recombinant plasmid to upregulate its expression. Among various circEZH2-targeting siRNAs (si-circEZH2-1 through si-circEZH2-5), si-circEZH2-1 was chosen for further studies due to its superior knockdown efficiency (Figure 2A). Post-transfection with the circEZH2 recombinant plasmid, a notable increase (48–61 fold) in circEZH2 expression was observed (Figure 2B). CCK-8 as well as colony formation detection indicated that reduced circEZH2 levels hindered, while increased levels promoted, A549 and SPC-A1 cell proliferation (Figure 2C and D). Additionally, an *in-vivo* study using a xenograft mouse model with A549 cells expressing circEZH2 and SPC-A1 cells with circEZH2 knockdown demonstrated the significant influence of circEZH2 on tumor growth, with overexpression leading to larger tumor sizes and weights, and knockdown showing the opposite effect (Figure 2E). Immunohistochemical staining experiments correlated with these findings, showing

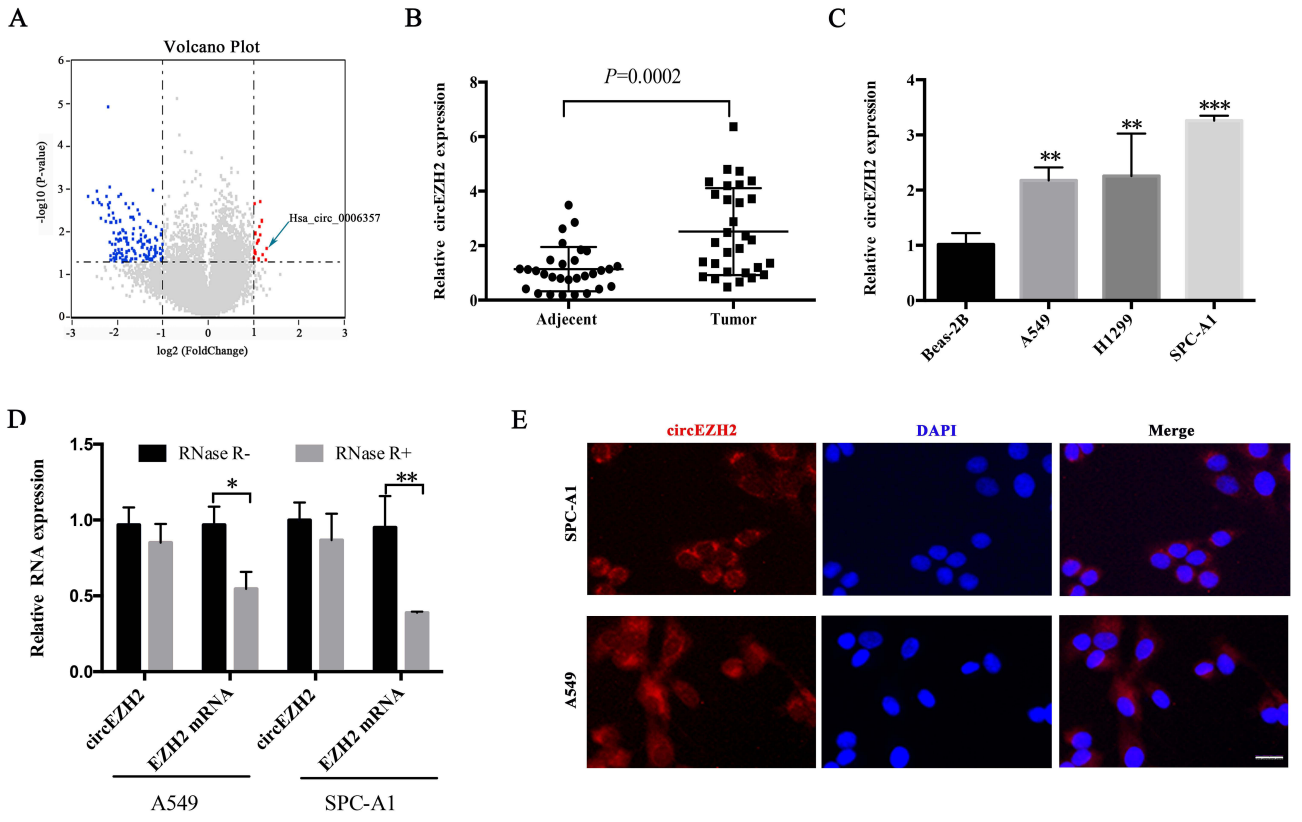

Figure 1 CircEZH2 is upregulated in lung adenocarcinoma (LUAD). (**A**) A comparative analysis using a circRNA microarray between LUAD and normal tissues identified hsa_circ_0006357 (circEZH2) as the most significantly elevated circRNA in LUAD samples. (**B** and **C**) Increased levels of circEZH2 were noted both in LUAD patient samples (n=30) and LUAD cell lines (A549, SPCA-1, and NCI-H1299), in contrast to BEAS-2B cells. (**D**) CircEZH2's stability against RNase R digestion was confirmed using RT-qPCR post-digestion. (**E**) FISH was employed to ascertain circEZH2's intracellular localization. CircEZH2 was indicated by red fluorescence, while nuclear DAPI staining appeared blue. The scale bar represents a distance of 50 μm. Statistical significance is indicated as *p<0.05, **p<0.01,***p<0.001. The presented data are from a minimum of three separate trials and are expressed as the mean±SD.

increased Ki-67 levels in samples with circEZH2 upregulation and decreased levels upon circEZH2 downregulation (Figure 2F). These results collectively suggest that circEZH2 plays a vital role in promoting LUAD cell proliferation and tumor growth.

CircEZH2 Promotes Migration, Invasion, and EMT of LUAD Cells

The influence of circEZH2 on LUAD cell invasion and migration was examined via wound healing assays and Transwell assays using SPC-A1 and A549 cells. The wound healing assays indicated a marked decrease in the healing rate upon circEZH2 knockdown, while its overexpression led to an enhanced healing rate (Figure 3A and B). Similarly, the Transwell assays showed a reduction in cell migration with circEZH2 knockdown and an increase with its overexpression (Figure 3C and D). Furthermore, immunoblotting analysis revealed that circEZH2 knockdown elevated the E-cadherin level as well as reduced vimentin and N-cadherin expression, which are markers of EMT. The reverse effects were noted upon circEZH2 overexpression (Figure 3E). These observations underscore the role of circEZH2 in augmenting the invasion, migration, and EMT process in LUAD cells.

CircEZH2 Augments Cellular Migration and Proliferation of LUAD Cells by Regulating miR-495-3p

The initial FISH analysis indicated a cytoplasmic prevalence of circEZH2, suggesting its role as an miRNA sponge. Using the CircBank and CircInteractome databases, four miRNAs potentially linked with circEZH2 were identified (Figure 4A). RNA pull-down assays with a biotin-labeled circEZH2 probe were then employed, demonstrating the preferential binding of circEZH2 over control oligonucleotides in lysates from A549 and SPC-A1 cells (Figure 4B). Subsequent RT-qPCR analysis revealed the substantial enrichment of miR-495-3p in these cells (Figure 4C). The

Table 1 Correlation Analysis Between Clinical Indications and circEZH2 Expression in LUAD Patients

Characteristics	n	circEZH2 level †		P value
		High	Low	
Total cases	30	15	15	
Gender				
Male	18	10	8	0.7104
Female	12	5	7	
Age (years)				
≤ 65	9	5	4	>0.999
>65	21	10	11	
Smoking history				
Yes	19	11	8	0.4497
No	11	4	7	
TNM stage				
I + II	24	9	15	0.0110*
III + IV	6	6	0	
Tumor size (cm)				
≤4	23	9	14	0.0801
>4	7	6	1	
Lymph node metastasis				
No	26	11	15	0.0996
Yes	4	4	0	

Notes: †Median expression level was used as cutoff. Low expression of circEZH2 in 30 patients was defined as a value below the 50th percentile, and high above the 50th percentile. P values were acquired by Fisher's test. *$P < 0.05$.

interaction site between circEZH2 and miR-495-3p was estimated through RNAalifold (http://rna.tbi.univie.ac.at/) (Figure 4D), and this interaction was verified by a dual-luciferase reporter system (Figure 4E and F). Further analyses showed reduced miR-495-3p expression in LUAD tissues compared to the adjacent nontumor tissues (Figure 4G), revealing a negative correlation between circEZH2 and miR-495-3p expression in LUAD tissues (Figure 4H). The overexpression of circEZH2 led to the downregulation of miR-495-3p, while its knockdown had the opposite effect (Figure 4I). These data support the assumption that circEZH2 may act as a sponge for miR-495-3p.

Rescue experiments assessed whether miR-495-3p modulates the circEZH2-induced cellular invasion, proliferation, and migration of LUAD cells. Colony formation and CCK-8 assays revealed that the suppressive effect of miR-495-3p overexpression on cell growth was mitigated by circEZH2 upregulation in A549 cells (Figure 5A and B). Wound healing and Transwell assays also demonstrated that miR-495-3p significantly reduced cell migration and invasion in A549 cells, but this suppression was counteracted by circEZH2 overexpression (Figure 5C and D). Furthermore, analysis of EMT markers showed that miR-495-3p overexpression in A549 cells enhanced the E-cadherin level and decreased the N-cadherin and vimentin levels. Remarkably, they were largely reversed by the overexpression of circEZH2 (Figure 5E). Thus, circEZH2 seems to drive cell migration, proliferation, and invasion by modulating miR-495-3p in LUAD cells.

CircEZH2 Elevates TPD52 Expression by Sponging miR-495-3p

Predictive analysis using the miRDB, TargetScan, miRTarBase, and StarBase databases identified 39 overlapping genes as potential targets of miR-495-3p (Figure 6A). Further selection from the StarBase database for genes inversely correlated with miR-495-3p in LUAD identified seven genes (*CNBP, MBTD1, NR6A1, R3HDM2, TPD52, UHMK1*, and *ZFAND5*) (Figure 6B). Upon transfecting miR-495-3p mimics into LUAD cells, RT-qPCR showed that the TPD52 mRNA levels were inversely affected (Figure 6C). Elevated TPD52 mRNA levels in LUAD cells tissues versus noncancerous tissues were

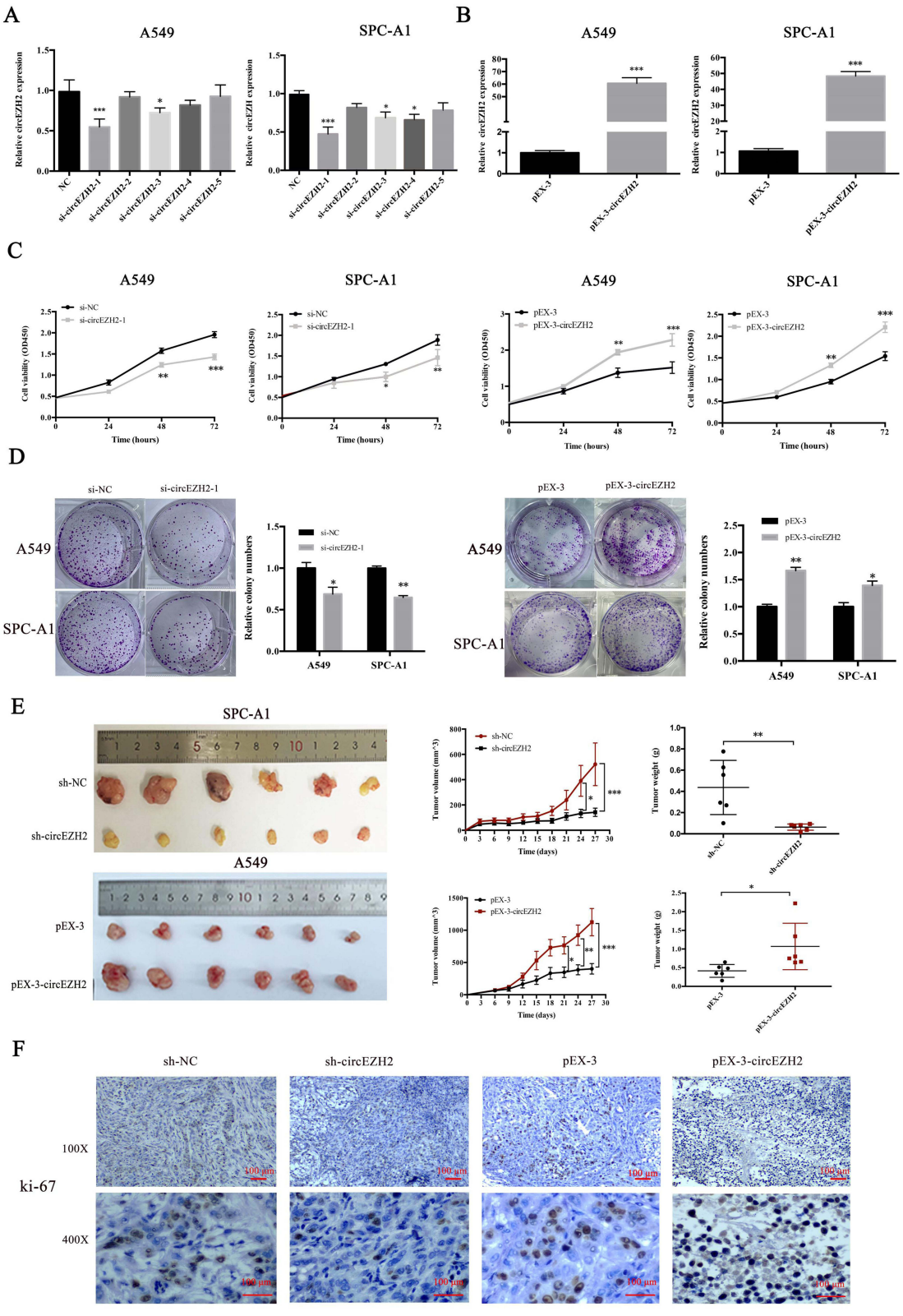

Figure 2 CircEZH2 is a driver of LUAD cell proliferation and tumor growth. (**A** and **B**) Post-transfection with siRNAs (si-circEZH2-1, si-circEZH2-2, si-circEZH2-3, si-circEZH2-4, and si-circEZH2-5) or pEX-3-circEZH2, circEZH2 expression was detected via RT-qPCR in LUAD cells. (**C**) The proliferation of LUAD cells treated with si-circEZH2-1 or pEX-3-circEZH2 was evaluated using CCK-8 assays. (**D**) The impact on lung cancer cell proliferation after transfection with si-circEZH2-1 or pEX-3-circEZH2 was examined through colony formation assays. (**E**) A comparative analysis of xenograft tumors, including growth curves and tumor weights, across different groups was performed (n=6). (**F**) Tumors from various groups underwent immunohistochemical staining to assess Ki-67 expression (scale bar=100 μm). Significance levels are indicated as *p<0.05, **p<0.01, ***p<0.001. The data are presented as the mean±SD, based on at least three independent assays.

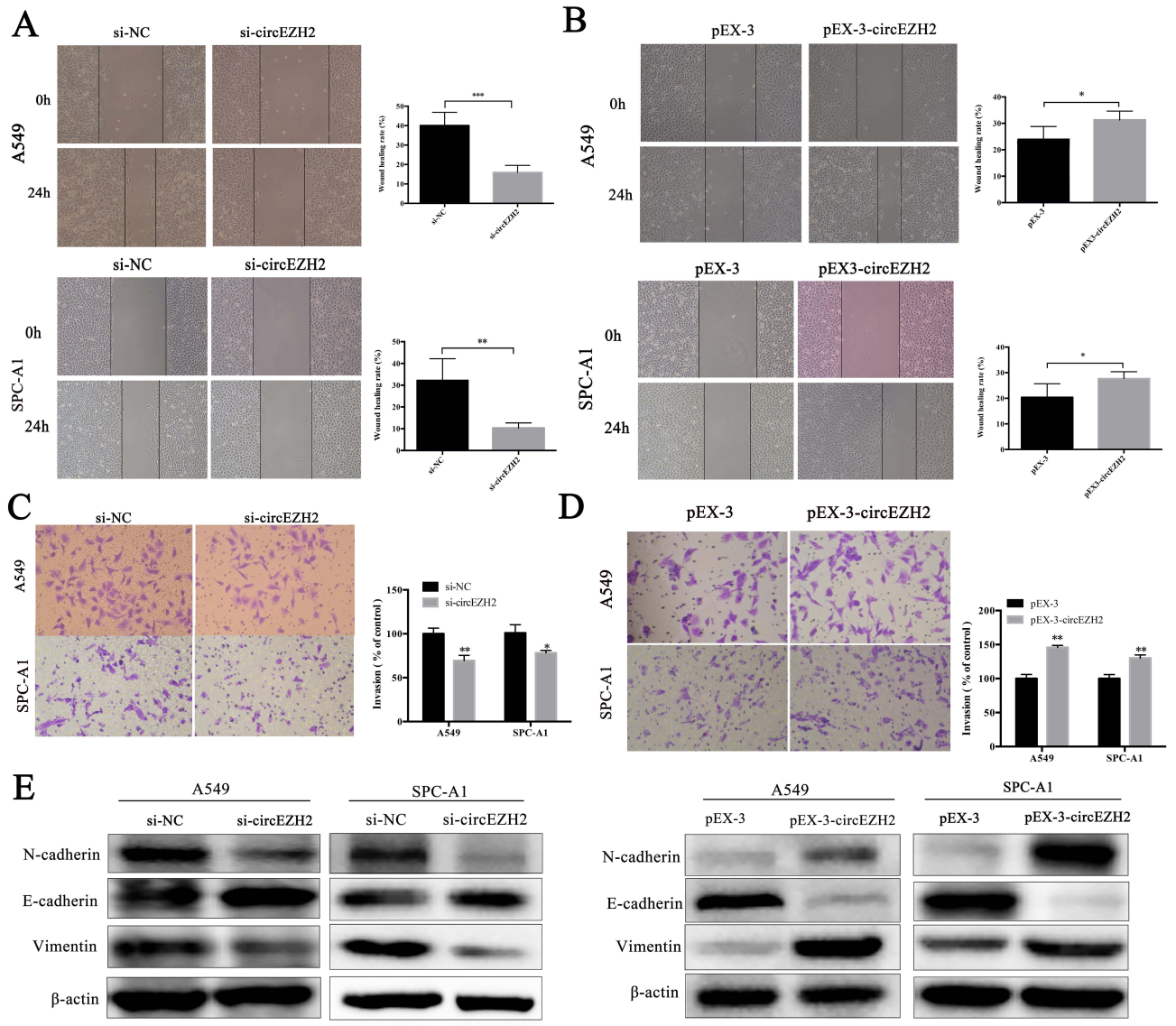

Figure 3 CircEZH2 enhances the invasion and migration capabilities of LUAD cells. (**A** and **B**) The migratory potential was gauged through wound healing assays using A549 and SPC-A1 cells post-transfection with si-circEZH2-1 or pEX-3-circEZH2 for 24 h. (**C** and **D**) The invasive capacity of these cells was ascertained using a Transwell assay. (**E**) To determine the level of EMT-related markers, an immunoblotting assay was conducted on the transfected LUAD cells. The levels of significance are marked as*p<0.05, **p<0.01, ***p<0.001. The results are presented as the mean±SD from a minimum of three separate experiments.

confirmed by RT-qPCR (Figure 6D). A negative correlation between TPD52 and miR-49-3p expression in cancerous tissues was found (Figure 6E). Immunoblotting analysis also revealed higher TPD52 protein levels in LUAD compared to the adjacent noncancerous tissue (Figure 6F). Furthermore, it was observed that circEZH2 overexpression significantly increased TPD52 expression, whereas its knockdown led to a reduction in TPD52 levels (Figure 6G). Notably, circEZH2 overexpression partially reversed the miR-495-3p-induced downregulation of TPD52 (Figure 6H).

CircEZH2/miR-495-3p/TPD52 Axis and Its Role in LUAD via the NF-κB Pathway

The NF-κB signaling pathway acts as a pivotal factor in the development and progression of LUAD, including tumor initiation.[14] A key component of this pathway is p65, which is a member of the NF-κB family that is known for its involvement in various cancer-related processes like cell invasion, survival, proliferation, angiogenesis, metastasis, and resistance to chemotherapy.[15] In this study, a decrease in the phosphorylated p65 (p-p65) levels in LUAD cells post circEZH2 knockdown was observed (Figure 7A), whereas circEZH2 overexpression led to increased p-p65 levels

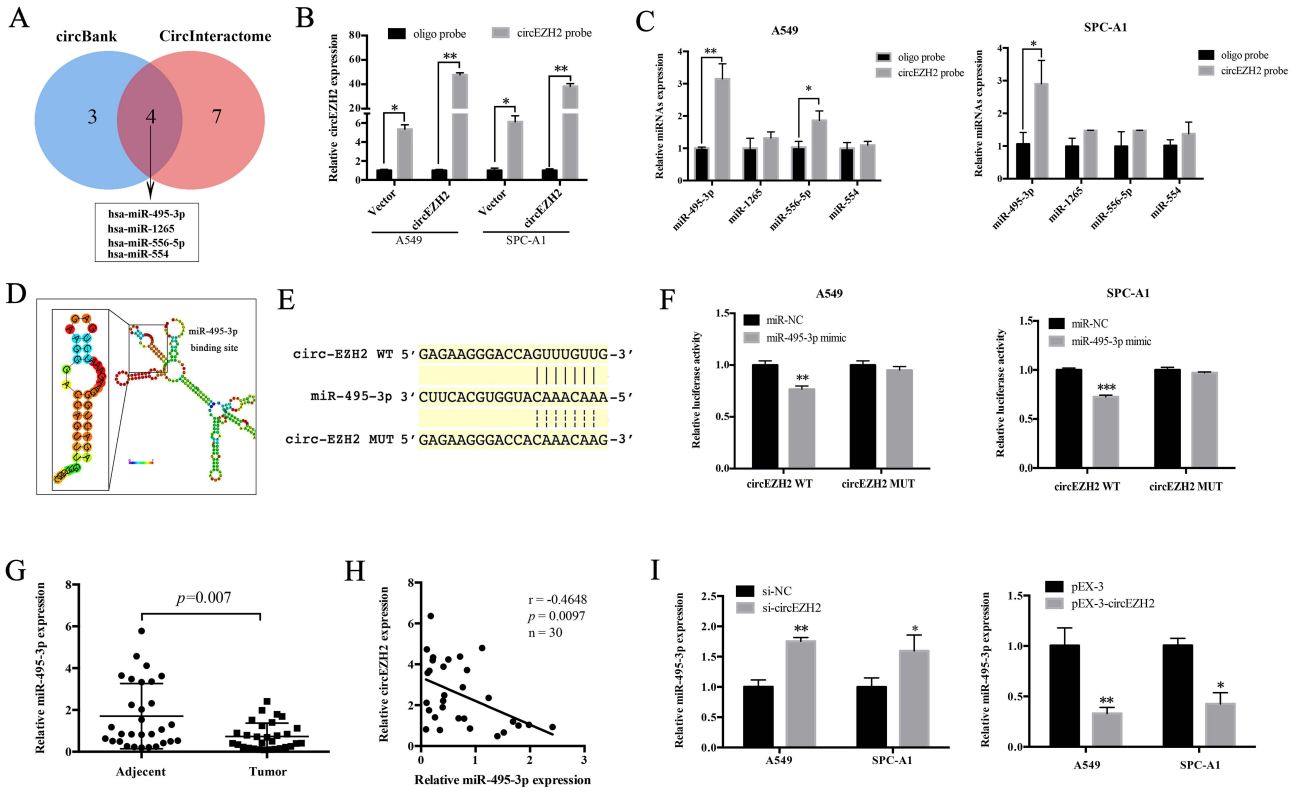

Figure 4 CircEZH2 works as a molecular sponge for miR-495-3p. (**A**) A Venn diagram was utilized to display shared target miRNAs of circEZH2, as forecasted by CircInteractome and circBank. (**B**) The performance of the circEZH2 probe was evaluated through an RNA pull-down assay followed by RT-qPCR. (**C**) Comparative analysis of four miRNAs in A549 and SPC-A1 cell lysates extracted using either circEZH2 or oligo probes. (**D**) An illustrative representation of circEZH2's secondary structure and potential miR-495-3p interaction sites as projected by RNAalifold. (**E** and **F**) The interaction between circEZH2-wild type (WT) and circEZH2-mutant (mut) (altered at the miR-495-3p binding site) was analyzed using luciferase reporter assays, in tandem with miR-495-3p mimics. (**G**) RT-qPCR was employed to measure the miR-495-3p levels in both adenocarcinoma and neighboring nontumorous tissues (n=30). (**H**) The association between miR-495-3p and circEZH2 in LUAD tissues was determined through Pearson's correlation analysis. (**I**) The levels of miR-495-3p were quantified via RT-qPCR in cells with either diminished or amplified circEZH2 expression. Significance markers: *p<0.05, **p<0.01, ***p<0.001. The data are presented as the mean±SD from a minimum of three separate experiments.

(Figure 7B). To explore the action of miR-495-3p within the NF-κB pathway, miR-495-3p mimics were introduced into A549 cells, resulting in reduced p-p65 expression. Notably, the overexpression of circEZH2 counteracted the miR-495-3p-induced decrease in p-p65 levels (Figure 7C). Additionally, the expression of p65 and p-p65 in LUAD tissue was assessed by immunoblotting analysis (Figure 7D), revealing a positive correlation between circEZH2 expression and NF-κB pathway activation in these tissues (Figure 7E).

Previous research has indicated that TPD52 can activate p65 within the NF-κB signaling cascade.[16] To examine the involvement of TPD52 in this pathway, three siRNAs targeting TPD52 were screened. The results showed that si-TPD52#1 and si-TPD52#3 effectively diminished TPD52 expression in LUAD cell lines (Figure 7F). Subsequent analysis revealed that TPD52 knockdown decreased p-p65 levels, while circEZH2 overexpression partially restored p-p65 expression (Figure 7G). In summary, these findings demonstrate that the circEZH2/miR-495-3p/TPD52 axis modulates the progression of LUAD by activating the NF-κB p65 signaling pathway (Figure 7H).

Discussion

LUAD is among the most prevalent malignant tumors globally, and its treatment remains inadequate, largely due to the absence of effective methods for early detection and intervention.[17] Research has increasingly highlighted the key role of circRNAs in the progression of various tumors.[18] For instance, hsa_circ_0049657 is downregulated in nonsmall cell lung cancer tissues and cells, and the overexpression of hsa_circ_0049657 may significantly suppress proliferation and invasion abilities as well as promote apoptosis.[19] Similarly, circ_0018414 has been identified as a suppressor of LUAD progression through its influence on the miR-6807-3p/DKK1 axis, which deactivates the Wnt/β-catenin

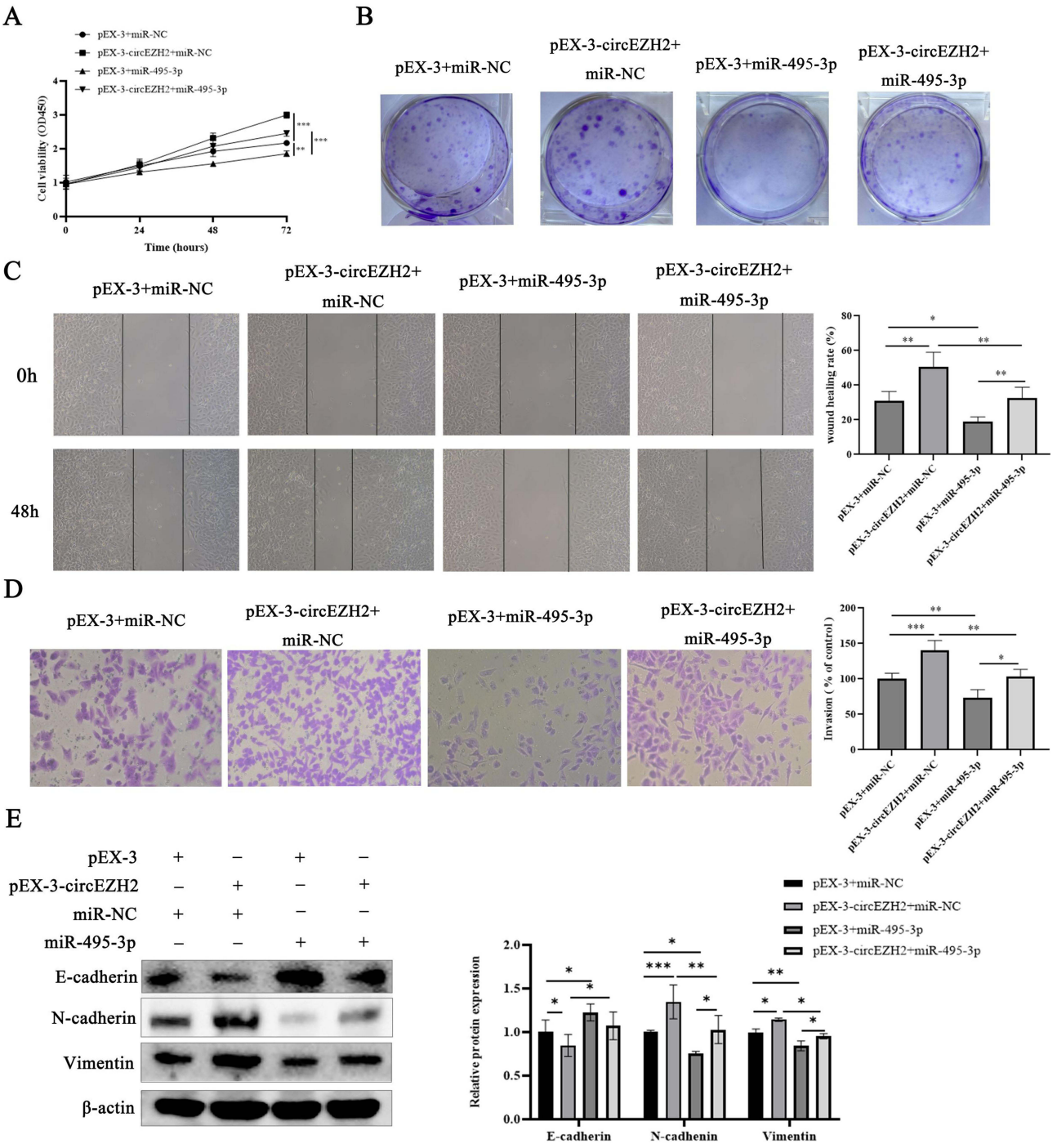

Figure 5 CircEZH2 enhances the proliferation, invasion, and migration of LUAD cells by inhibiting miR-495-3p. A549 cells underwent transfection with pEX-3+miR-NC, pEX-3+miR-495-3p, pEX-3-circEZH2+miR-NC, or pEX-3-circEZH2+miR-495-3p. (**A** and **B**) The proliferative capacity of A549 cells was examined by using both colony formation and CCK-8 assays. (**C** and **D**) The invasion and migration traits of A549 cells were examined through Scratch and Transwell assays, respectively. (**E**) The protein levels of E-cadherin, N-cadherin, and vimentin in these cells were determined using Western blotting techniques. Significance levels are revealed as *p<0.05, **p<0.01, ***p<0.001. All reported data are presented as the mean±SD, derived from at least three separate studies.

pathway.[20] This study demonstrates that circEZH2 controls LUAD cell migration, proliferation, as well as invasion in vitro. Additionally, it was observed that circEZH2 accelerated tumor growth in vivo. Hence, these findings underscore the action of circEZH2 in advancing the progression of LUAD.

Growing evidence suggests that circRNAs can act as competitive endogenous RNAs (ceRNAs), sequestering miRNAs and thereby modulating the expression of miRNAs and their target genes.[21] The mechanism of action of

A

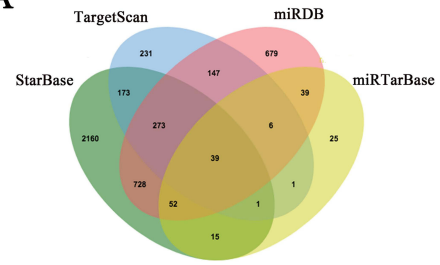

Overlapped genes were found from four databases							
RUNX3	ANKRD1	TNFRSF1B	HIPK1	UHMK1	CELF2	DDIT4	BDNF
KIAA154	R3HDM2	IGF1	RIMKLB	DICER1	NRXN3	NUFIP2	MBTD1
CRLS1	MIEF1	ATP2B2	VGLL4	CNBP	U2SURP	PDLIM5	FEM1C
BCAP29	TPD52	MOB3B	ZFAND5	NR6A1	RORB	RPS6KA3	KLHL15
CADM1	ATRN	CDK6	SESN3	PER2	THBS2	ZFX	

B

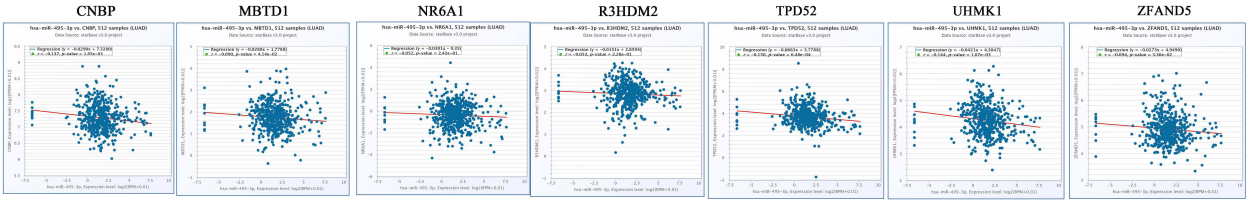

C

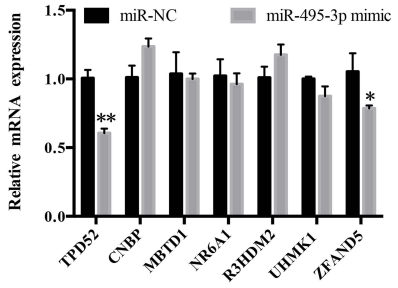

D

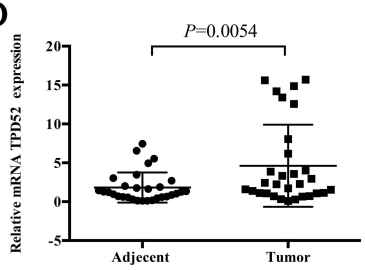

E

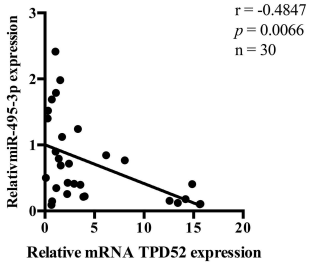

F

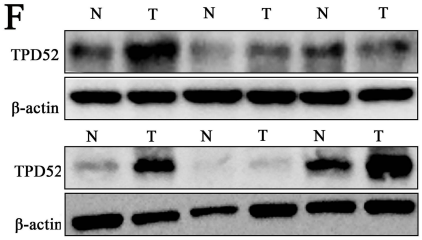

G

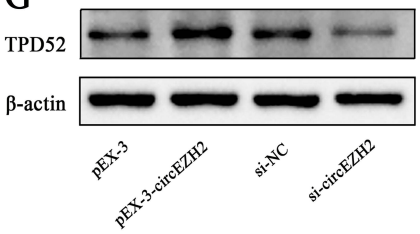

H

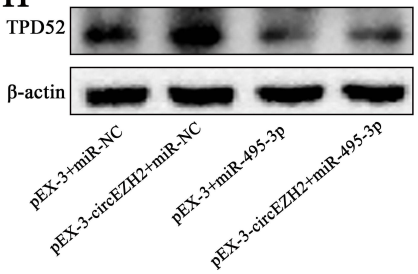

Figure 6 CircEZH2 modulates miR-495-3p to increase TPD52 expression. (**A**) Prediction of miR-495-3p's target genes was conducted using databases such as StarBase, miRTarBase, TargetScan, and miRDB, revealing overlapping targets. (**B**) Pearson correlation analysis was performed to examine the relationship of miR-495-3p with genes including *CNBP, MBTD1, NR6A1, R3HDM2, TPD52, UHMK1*, and *ZFAND5*, as cataloged in StarBase. (**C**) Following transfection in A549 cells, changes in mRNA expression were observed. (**D**) The mRNA levels of TPD52 in LUAD tissues and adjacent healthy tissues (n=30) were quantified via RT-qPCR. (**E**) A correlation study between miR-495-3p and TPD52 mRNA in LUAD tissues was conducted. (**F**) The levels of protein expression of TPD52 in LUAD and the surrounding nonmalignant tissues (n=6) were investigated by immunoblotting assays. (**G** and **H**) Post-transfection TPD52 protein concentrations in A549 cells were assessed by immunoblotting assays. Statistical significance is denoted as *p<0.05, **p<0.01. Data are presented as the mean±SD from a minimum of three separate assays.

circRNAs is intricately associated with their subcellular distribution.[22] This research demonstrated that circEZH2 predominantly resided in the cytoplasm and that miR-495-3p significantly diminishes the luciferase activity of circEZH2. Known as a tumor suppressor in the genesis and evolution of tumors, miR-495-3p impedes the migration and proliferation of colorectal cancer cells by targeting and reducing the levels of the high mobility group box 1 protein.[23] Additionally, miR-495-3p can trigger lethal mitophagy in nonsmall cell lung cancer by altering the sphingolipid balance towards ceramide, targeting sphingosine kinase 1.[24] In this study, miR-495-3p was found to be less expressed in LUAD tissues compared to normal tissues, and its expression was inversely correlated with the circEZH2 levels. Moreover, it was observed that miR-495-3p mitigated the impact of circEZH2, reversing the effects of circEZH2

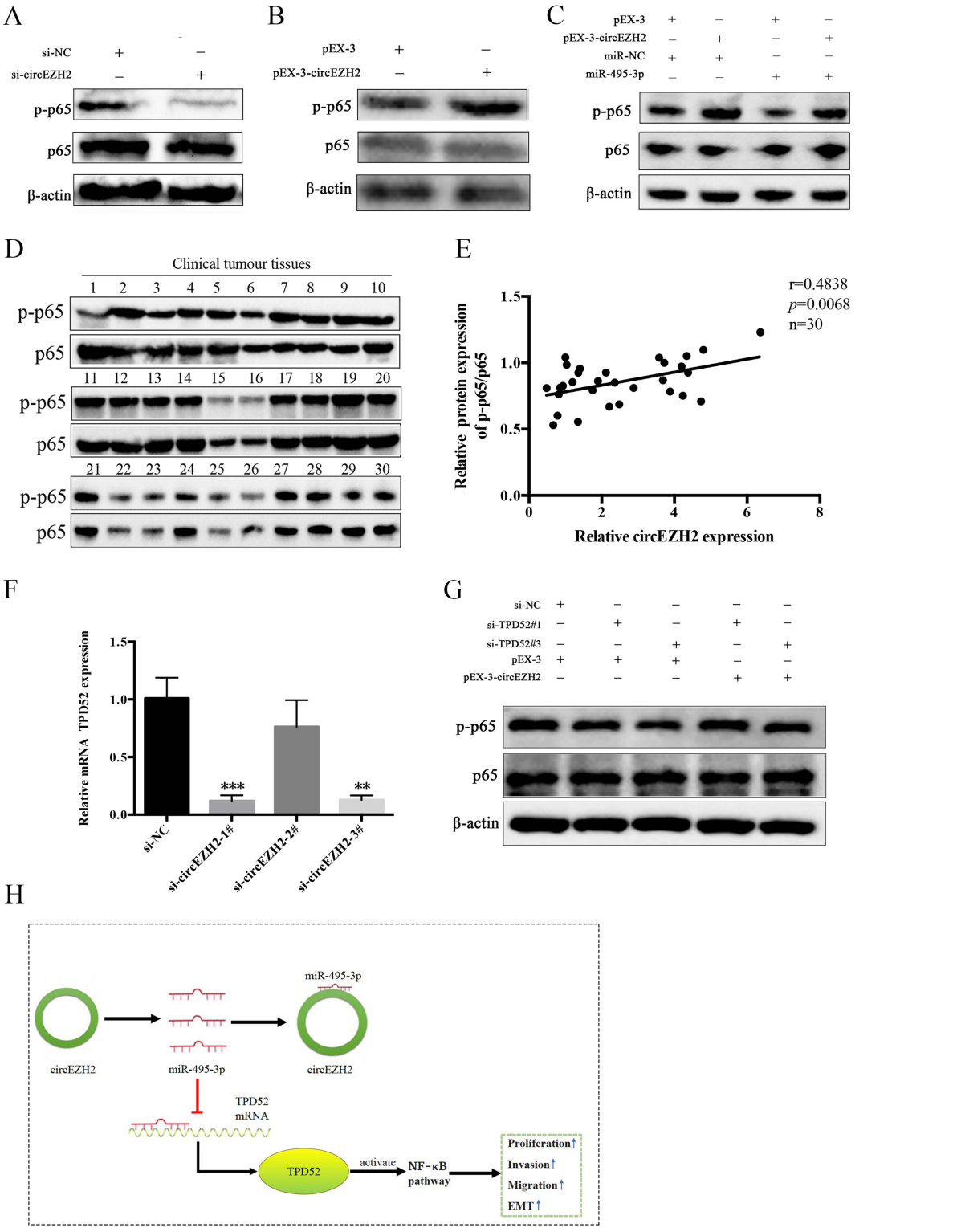

Figure 7 The circEZH2/miR-495-3p/TPD52 axis contributes to LUAD development via the NF-κB pathway. (**A**) The protein levels of p-p65 and p65 in LUAD cells were determined by Western blot following si-circEZH2 transfection. (**B**) Cells transfected with pEX-3-circEZH2 underwent similar analysis. (**C**) Examination of p-p65 and p65 protein levels in A549 cells transfected with both miR495-3p and pEX-3-circEZH2 was performed. (**D**) Immunoblotting assays were conducted to verify the protein expression of p-p65 and p65 in clinical tumor tissues (n=30). (**E**) The correlation between circEZH2 and p-p65/p65 in LUAD tissues was determined by Pearson's correlation analysis. (**F**) Post-transfection with siRNAs targeting TPD52 (TPD52#1, TPD52#2, and si-TPD52#3), TPD52 expression in A549 cells was measured using RT-qPCR. (**G**) The influence of si-TPD52#1/si-TPD52#3 in combination with pEX-3-circEZH2 on p-p65 and p65 protein expression was assessed in A549 cells by immunoblotting assays. (**H**) A schematic representation was created to depict the regulatory role of the circEZH2/miR-495-3p/TPD52 axis in promoting LUAD cell proliferation and metastasis. Statistical significance is denoted as $^{**}p<0.01$, $^{***}p<0.001$. Data are presented as the mean±SD from a minimum of three separate assays.

on the migration, proliferation, and invasion of LUAD cells. Therefore, these results suggest that the oncogenic effects of circEZH2 in LUAD might be through sponging miR-495-3p.

TPD52 is recognized as a cancer-promoting gene in human malignancies, exhibiting heightened expression in different types of cancers such as squamous cell lung cancer,[25] breast cancer,[26] pancreatic cancer,[27] and cervical cancer.[28] In the current study, TPD52 expression was found to be elevated in LUAD tissues, and its expression was inversely correlated with the miR-495-3p levels. The presence of circEZH2 significantly reduced the influence of miR-495-3p on TPD52 expression. These outcomes suggest that in LUAD, circEZH2 potentially operates as a ceRNA for miR-495-3p, thereby regulating TPD52 expression.

Emerging studies indicate that various circRNAs can influence the NF-κB pathway in different cancers.[29,30] Dysregulated activation of NF-κB is a common feature in several cancers,[31] including lung cancer.[32] The current study reveals that circEZH2 enhances TPD52 expression by sequestering miR-495-3p, which in turn activates the NF-κB signaling pathway, fostering the progression of LUAD. This aligns with findings from prior research in this area.

Although the role of the miR-495-3p/TPD52 axis in circEZH2-mediated function was evident, the results do not exclude the possibility that circEZH2 may be involved in other regulatory mechanisms or interact with additional miRNA/mRNA/protein targets not yet investigated. It is also evident from various research that circRNAs can bind to RNA-binding proteins, an important characteristic that can reveal more about the functions of circRNAs. For instance, studies have shown that circEZH2 interacts with the m6A reader IGF2BP2, preventing its ubiquitin-dependent degradation.[33] Future investigations are planned to explore additional potential functions and interactions of circEZH2 in LUAD, particularly its association with RNA-binding proteins.

In addition, recent studies have found that the concordance rate of differentially expressed mRNAs and proteins in LUAD patients may be related to ethnicity.[34] Differences in genetic backgrounds, including single nucleotide polymorphisms (SNPs) and genetic variations, can impact post-transcriptional processes and protein synthesis efficiency. Differences in the genetic background may also affect the biogenesis and regulatory mechanisms of circRNAs. For example, specific SNPs associated with certain racial groups may alter the processing or stability of circRNAs, leading to differences in expression patterns between populations.[35] Currently, there is limited information on the differences in circRNA expression in LUAD among different ethnic groups, and the mechanisms and clinical implications are not yet fully understood. Thus, further studies are warranted.

Conclusion

This study introduces a novel action of the circRNA circEZH2, which is markedly overexpressed in LUAD tissues and cell lines. Functionally, circEZH2 enhances cellular migration, proliferation, and invasion. It acts as a ceRNA for miR-495-3p, influencing TPD52 expression and triggering the NF-κB signaling pathway.

Ethics Approval and Consent to Participate

This study was performed in line with the principles of the Declaration of Helsinki. Approval was granted by the Ethics Committee of the Affiliated People's Hospital of Ningbo University (approval number: 2022012). All animal experimental protocols were approved by the Animal Experimental Research Ethics Committee of Ningbo University (approval number: 11332), and all experimental procedures followed the Guidelines of the Care and Use of Laboratory Animals issued by the Chinese Council on Animal Research. This study was performed in compliance with the ARRIVE ESSENTIAL 10 guidelines.

Acknowledgments

We thank Jianbo Wen and Kefeng Huang for their help in collecting tissue specimens.

Funding

This work was supported by the Natural Science Foundation of Ningbo (Grant numbers: 2022J032 and 2023J387), a Medical Science and Technology Project of Zhejiang Province (Grant number: 2024KY370), a Ningbo Leading

Medical & Health Discipline grant (Grant number: 2022-B19), and the National Natural Science Foundation of China (Grant number: 81872433).

Disclosure

The authors report no conflicts of interest in this work.

References

1. Li F, Wang S, Wang Y, et al. Multi-omics analysis unravels the underlying mechanisms of poor prognosis and differential therapeutic responses of solid predominant lung adenocarcinoma. *Front Immunol*. 2023;14:1101649. doi:10.3389/fimmu.2023.1101649
2. Kristensen LS, Andersen MS, Stagsted LVW, Ebbesen KK, Hansen TB, Kjems J. The biogenesis, biology and characterization of circular RNAs. *Nat Rev Genet*. 2019;20(11):675–691. doi:10.1038/s41576-019-0158-7
3. Wang C, Tan S, Li J, Liu WR, Peng Y, Li W. CircRNAs in lung cancer - Biogenesis, function and clinical implication. *Cancer Lett*. 2020;492:106–115. doi:10.1016/j.canlet.2020.08.013
4. Wang C, Tan S, Liu WR, et al. RNA-Seq profiling of circular RNA in human lung adenocarcinoma and squamous cell carcinoma. *Mol Cancer*. 2019;18(1):134. doi:10.1186/s12943-019-1061-8
5. Liu Y, Zhang H, Zhang W, et al. circ_0004140 promotes LUAD tumor progression and immune resistance through circ_0004140/miR-1184/CCL22 axis. *Cell Death Discov*. 2022;8(1):181. doi:10.1038/s41420-022-00983-w
6. Liu X, Feng Y, Wang L, et al. Silencing of circ_0088036 inhibits growth and invasion of lung adenocarcinoma through miR-203/SP1 axis. *J Biochem Mol Toxicol*. 2024;38(4):e23684. doi:10.1002/jbt.23684
7. Zhao M, Feng J, Tang L. Competing endogenous RNAs in lung cancer. *Cancer Biol Med*. 2021;18(1):1–20. doi:10.20892/j.issn.2095-3941.2020.0203
8. Wang J, Zhao X, Wang Y, et al. circRNA-002178 act as a ceRNA to promote PDL1/PD1 expression in lung adenocarcinoma. *Cell Death Dis*. 2020;11(1):32. doi:10.1038/s41419-020-2230-9
9. Li Y, Li F, Feng C, et al. MiR-372-3p functions as a tumor suppressor in colon cancer by targeting MAP3K2. *Front Genet*. 2022;13:836256. doi:10.3389/fgene.2022.836256
10. Cheng Z, Yu C, Cui S, et al. circTP63 functions as a ceRNA to promote lung squamous cell carcinoma progression by upregulating FOXM1. *Nat Commun*. 2019;10(1):3200. doi:10.1038/s41467-019-11162-4
11. Shang C, Li Y, He T, et al. The prognostic miR-532-5p-correlated ceRNA-mediated lipid droplet accumulation drives nodal metastasis of cervical cancer. *J Adv Res*. 2022;37:169–184. doi:10.1016/j.jare.2021.09.009
12. Wang H, Si S, Jiang M, Chen L, Huang K, Yu W. Leukemia inhibitory factor is involved in the pathogenesis of NSCLC through activation of the STAT3 signaling pathway. *Oncol Lett*. 2021;22(3):663. doi:10.3892/ol.2021.12924
13. Livak KJ, Schmittgen TD. Analysis of relative gene expression data using real-time quantitative PCR and the 2(-Delta Delta C(T)) Method. *Methods*. 2001;25(4):402–408. doi:10.1006/meth.2001.1262
14. Chen H, Chen X, Pan B, Zheng C, Hong L, Han W. KRT8 serves as a novel biomarker for LUAD and promotes metastasis and EMT via NF-kappaB signaling. *Front Oncol*. 2022;12:875146. doi:10.3389/fonc.2022.875146
15. Taniguchi K, Karin M. NF-kappaB, inflammation, immunity and cancer: coming of age. *Nat Rev Immunol*. 2018;18(5):309–324. doi:10.1038/nri.2017.142
16. Dasari C, Yaghnam DP, Walther R, Ummanni R. Tumor protein D52 (isoform 3) contributes to prostate cancer cell growth via targeting nuclear factor-kappaB transactivation in LNCaP cells. *Tumour Biol*. 2017;39(5):1010428317698382. doi:10.1177/1010428317698382
17. Spella M, Stathopoulos GT. Immune resistance in lung adenocarcinoma. *Cancers*. 2021;13(3):384. doi:10.3390/cancers13030384
18. Su L, Zhao J, Su H, et al. CircRNAs in lung adenocarcinoma: diagnosis and therapy. *Curr Gene Ther*. 2022;22(1):15–22.
19. Ren Y, Zhao Y, Shan Y, et al. Circular RNA hsa_circ_0049657 as a potential biomarker in non-small cell lung cancer. *Int J Mol Sci*. 2023;24(17):13237. doi:10.3390/ijms241713237
20. Yao Y, Zhou Y, Hua Q. circRNA hsa_circ_0018414 inhibits the progression of LUAD by sponging miR-6807-3p and upregulating DKK1. *Mol Ther Nucleic Acids*. 2021;23:783–796. doi:10.1016/j.omtn.2020.12.031
21. Tang X, Ren H, Guo M, Qian J, Yang Y, Gu C. Review on circular RNAs and new insights into their roles in cancer. *Comput Struct Biotechnol J*. 2021;19:910–928. doi:10.1016/j.csbj.2021.01.018
22. Kristensen LS, Jakobsen T, Hager H, Kjems J. The emerging roles of circRNAs in cancer and oncology. *Nat Rev Clin Oncol*. 2022;19(3):188–206. doi:10.1038/s41571-021-00585-y
23. Zhang JL, Zheng HF, Li K, Zhu YP. miR-495-3p depresses cell proliferation and migration by downregulating HMGB1 in colorectal cancer. *World J Surg Oncol*. 2022;20(1):101. doi:10.1186/s12957-022-02500-w
24. Arora S, Singh P, Tabassum G, Dohare R, Syed MA. miR-495-3p regulates sphingolipid metabolic reprogramming to induce Sphk1/ceramide mediated mitophagy and apoptosis in NSCLC. *Free Radic Biol Med*. 2022;189:71–84. doi:10.1016/j.freeradbiomed.2022.07.001
25. Kumamoto T, Seki N, Mataki H, et al. Regulation of TPD52 by antitumor microRNA-218 suppresses cancer cell migration and invasion in lung squamous cell carcinoma. *Int J Oncol*. 2016;49(5):1870–1880. doi:10.3892/ijo.2016.3690
26. Chen Y, Peng C, Tan W, et al. Tumor protein D52 (TPD52) affects cancer cell metabolism by negatively regulating AMPK. *Cancer Med*. 2023;12(1):488–499. doi:10.1002/cam4.4911
27. Wang Z, Li Y, Fan L, et al. Silencing of TPD52 inhibits proliferation, migration, invasion but induces apoptosis of pancreatic cancer cells by deactivating Akt pathway. *Neoplasma*. 2020;67(2):277–285. doi:10.4149/neo_2019_190404N295
28. Shi P, Zhang X, Lou C, Xue Y, Guo R, Chen S. Hsa_circ_0084927 regulates cervical cancer advancement via regulation of the miR-634/TPD52 Axis. *Cancer Manag Res*. 2020;12:9435–9448. doi:10.2147/CMAR.S272478
29. Meng F, Zhang X, Wang Y, et al. Hsa_circ_0021727 (circ-CD44) promotes ESCC progression by targeting miR-23b-5p to activate the TAB1/NFkappaB pathway. *Cell Death Dis*. 2023;14(1):9. doi:10.1038/s41419-022-05541-x

30. Xu Y, Zhang S, Liao X, et al. Circular RNA circIKBKB promotes breast cancer bone metastasis through sustaining NF-kappaB/bone remodeling factors signaling. *Mol Cancer*. 2021;20(1):98. doi:10.1186/s12943-021-01394-8
31. Dolcet X, Llobet D, Pallares J, Matias-Guiu X. NF-kB in development and progression of human cancer. *Virchows Arch*. 2005;446(5):475–482. doi:10.1007/s00428-005-1264-9
32. Dimitrakopoulos FD, Kottorou AE, Kalofonou M, Kalofonos HP. The fire within: NF-kappaB involvement in non-small cell lung cancer. *Cancer Res*. 2020;80(19):4025–4036. doi:10.1158/0008-5472.CAN-19-3578
33. Yao B, Zhang Q, Yang Z, et al. CircEZH2/miR-133b/IGF2BP2 aggravates colorectal cancer progression via enhancing the stability of m(6) A-modified CREB1 mRNA. *Mol Cancer*. 2022;21(1):140. doi:10.1186/s12943-022-01608-7
34. Liu Y, Li Z, Meng Q, et al. Identification of the consistently differential expressed hub mRNAs and proteins in lung adenocarcinoma and construction of the prognostic signature: a multidimensional analysis. *Int J Surg*. 2024;110(2):1052–1067. doi:10.1097/JS9.0000000000000943
35. López-Jiménez ZE, Andrés-León E. The implications of ncrnas in the development of human diseases. *Non-Cod RNA*. 2021;7(1):17. doi:10.3390/ncrna7010017